



## Simulation of the cosmic ray Moon shadow in the geomagnetic field

Giuseppe Di Sciascio<sup>a</sup>, Roberto Iuppa<sup>a,b,\*</sup>

<sup>a</sup> INFN, Sez. Roma Tor Vergata, Rome, Italy

<sup>b</sup> Dipartimento di Fisica, Università Roma Tor Vergata, Rome, Italy

### ARTICLE INFO

Available online 22 June 2010

#### Keywords:

Cosmic rays

Extensive air shower

Monte Carlo simulations

Moon shadow

### ABSTRACT

An accurate Monte Carlo simulation of the deficit of primary cosmic rays in the direction of the Moon has been developed to interpret the observations reported in the TeV energy region until now. Primary particles are propagated through the geomagnetic field in the Earth–Moon system. The algorithm is described and the contributions of the detector resolution and of the geomagnetic field are disentangled.

© 2010 Elsevier B.V. All rights reserved.

### 1. Introduction

Since the galactic cosmic rays are hampered by the Moon, a deficit of cosmic rays in its direction is expected (the so-called “Moon shadow”). The Moon shadow is an important tool to calibrate the performance of an air shower array. In fact, the size of the deficit allows a measurement of the angular resolution and the position of the deficit allows the evaluation of the absolute pointing accuracy of the detector.

In addition, the Earth–Moon system acts as a magnetic spectrometer deflecting the charged cosmic rays by an angle inversely proportional to their energy. The observation of such a displacement provides a direct check of the relation between shower size and primary energy, thus calibrating the detector.

This effect allows, in principle, the search of antiparticles in the opposite direction of the observed Moon shadow being paths of primary antiprotons deflected in an opposite sense in their way to the Earth.

A detailed Monte Carlo simulation of cosmic ray propagation in the Earth–Moon system is mandatory to understand the Moon shadow phenomenology and to compare the observed westward displacement with the expectations in order to disentangle the geomagnetic effect from some possible experimental biases.

### 2. Monte Carlo simulation

#### 2.1. Simulation strategy

When the emission of photons by a given gamma-ray source has to be simulated, a classical approach can be followed: once its energy spectrum is known, it is enough to decide for how long the

source emission has to be reproduced to calculate the number of expected events which have to be sampled. Of course, if the response of an Earth-based array has to be simulated, for each one of these primary particles also induced shower and the detector response have to be calculated. The easiest way to do that is to shoot up the particles from the detector<sup>1</sup> to the source. This trick allows to concentrate the efforts of the simulation only on the showers which effectively construct the signal.

Nonetheless, this method cannot be used for the Moon shadow as it is, because of two main reasons.

1. The Moon shadow is not a signal, but a “lack” in the background.
2. The effect is provoked by charged particles and not by photons. This implies that we must take into account the effect of the electro-magnetic fields on their trajectories.

The first argument is the more relevant one. In fact, if we wanted to remain faithful to the approach of simulating only the particles which reach the detector, we should compute the showers of the background surrounding the Moon and then take off the ones coming exactly from within Moon. In such terms, the simulation is likely unfeasible, at least for low energy threshold experiments. To be precise, if the detector energy threshold is a few hundreds of GeV, even by considering a square sky window surrounding the Moon not so large (e.g. 10°), too many showers should have to be simulated to reproduce even just one year of data taking.

It is evident that the Moon shadow requires a different strategy of simulation. It is better to treat the Moon like a standard source and then reverse the amplitude of the signal. In the end, both the gamma-source case and the Moon shadow case

\* Corresponding author at: INFN, Sez. Roma Tor Vergata, Rome, Italy.

E-mail addresses: [disciascio@roma2.infn.it](mailto:disciascio@roma2.infn.it) (G. Di Sciascio), [iuppa@roma2.infn.it](mailto:iuppa@roma2.infn.it) (R. Iuppa).

<sup>1</sup> Actually, from a suitably-chosen area around it.

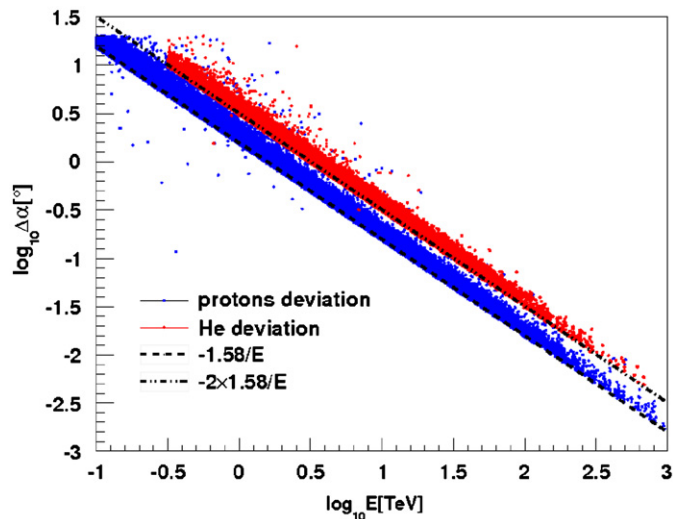


**Fig. 1.** Deviation induced by the geomagnetic field on protons and He nuclei. Each point refers to a simulated shower. Both the arrival direction and the date of the propagation are randomly sampled, respectively, from an isotropic distribution within the sky and from a uniform distribution over 2008. The analytical trends obtained from Eq. (1) are also shown.

reduce to a perturbation of the cosmic-rays background. The only difference is the sign of the perturbation.

Because of their electric charge the cosmic rays do not proceed straight from the Moon to the Earth, but their trajectories are bent by the geomagnetic field. Since this effect plays a crucial role in the final result of the physics analysis, it must not be underestimated during the simulation. Especially for those particles which have low energy, the bending effect is very strong and a realistic prediction is possible only if the simulation accounts correctly for the intensity and the direction of the geomagnetic field. What is more, notice that when the particles are sent back to the Moon from the detector, the sign of their charge must be reversed to properly reproduce the direction of the deviation.

## 2.2. The simulation of an ideal detector

The air showers development in the atmosphere has been generated with the CORSIKA v. 6.500 code including the QGSJET-II.03 hadronic interaction model [1]. Cosmic ray spectra have been simulated in the energy range from 30 GeV to 1 PeV following the relative normalization given in Ref. [2], resulting from a global fit of main experimental data. About  $10^8$  showers have been sampled in the zenith angle interval  $0-60^\circ$ . The secondary electromagnetic component has been propagated down to a cut-off energy of 1 MeV.

At present, the only experiment able to observe the Moon shadow with high statistical significance at an energy threshold well below 1 TeV is ARGO-YBJ [3]. Therefore, we simulated, via a GEANT4-based code [4], an ideal detector placed in YangBajing (4300 m a.s.l.) having geometrical features similar to ARGO-YBJ and a duty-cycle of 90%. The shower core positions have been randomly sampled in an energy-dependent area large up to  $10^3 \times 10^3 \text{ m}^2$ , centered on the detector. We analyzed all events with more than 20 charged particles over the whole detector.

## 2.3. The geomagnetic model

It has been already noticed that if a primary cosmic ray (energy  $E$ , charge  $Z$ ) traversing the geomagnetic field is observed by a detector placed in YangBajing, its trajectory shows a deviation

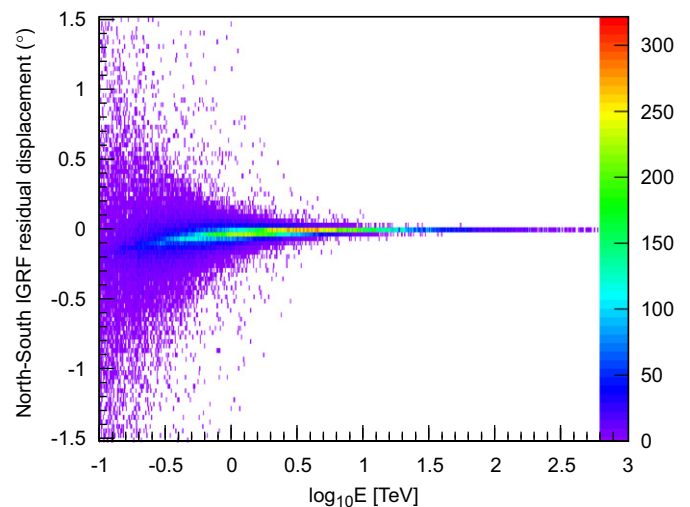
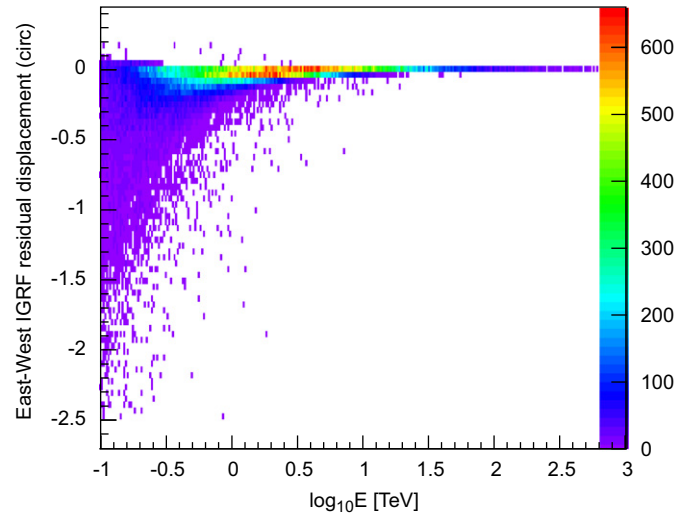


**Fig. 2.** Residual displacement with respect to the analytical expectation. The deviation is calculated by applying the T-IGRF model (see text). The color scale represents the number of showers laying on the single pixel. (For interpretation of the references to color in this figure legend, the reader is referred to the web version of this article.)

along the East–West direction [5]<sup>2</sup> which in first approximation can be written as

$$\Delta\vartheta \simeq -1.58^\circ \frac{Z}{E[\text{TeV}]} \quad (1)$$

The sign is set according to the usual way to represent the East–West projection of the Moon maps (see Fig. 3). Eq. (1) can be easily derived by assuming that the geomagnetic field is provoked by a pure dipole laying in the centre of the Earth (see Appendix). Nonetheless this approximation, which is derived for nearly vertical primaries, is not enough when the primaries energy is below few TeV.

To perform a numerical estimate of the bending effect, it is necessary to adopt a model of the magnetic field in the Earth–Moon system. The roughest one is the so-called Virtual Dipole Model (VDM), whose name is self-explaining. A better choice is the Tsyganenko-IGRF model (T-IGRF hereafter) [6], which accounts for both internal and external magnetospheric sources.

<sup>2</sup> No deviation is expected along the North–South one.

We compared the effect on the particle trajectories of VDM and T-IGRF, in both cases finding non-negligible differences with respect to the  $-1.58^\circ Z/E(\text{TeV})$  formula. Among the two models themselves, we observed discrepancies up to the  $\sim 15\%$  level ( $4-7^\circ$ ) for sub-TeV primary energies, mainly due to the field intensity near the Earth surface. Since the T-IGRF model accounts for more factors, we refer to it hereafter. In Fig. 1, you can appreciate the analytical trend (Eq. (1)) together with the actual East–West displacement calculated applying the T-IGRF model for protons and He nuclei. The analytical approach clearly underestimates the East–West deviation.

Fig. 2 shows the differences of the T-IGRF-induced deviation with respect to the leading term  $1.58^\circ Z/E(\text{TeV})$ . The upper (lower) panel contains such a residual deviation along the East–West (North–South) direction as a function of the primary energy. Although there are no effects for energies  $E > 10 \text{ TeV}$ , below few TeV the residual displacement can reach  $1^\circ$ . Notice that unlike the analytical approach would suggest, the North–South deviation of the single primary is non-null, being zero only on average.

#### 2.4. Moon shadow simulation

By following the procedure described before, we can obtain the Moon shadow maps represented in Fig. 3. There can be appreciated the displacement induced by the geomagnetic field.

The long tail of the left part of the up-right map is made by the lowest energy particles (below 1 TeV) which are more deviated. Concerning the bottom-left map, the detector by itself provides the smearing of the signal, leaving intact the circular symmetry, as expected.

It is possible to study the effects of the finite angular resolution of the detector and of the geomagnetic field separately.

As already noticed, if we consider the magnetic deviation but not the detector, the circular symmetry of the signal is broken only along the East–West direction (see Fig. 3, top-right map). That make us confident that only the smearing due to the angular resolution affects the signal along the north–south direction, thus allowing its determination. Actually, we stress that what we determine by considering the spread of the signal along the North–South direction, cannot be properly named angular resolution, because the Moon is not a point-like source and its own finite angular width (half a degree) contributes to the spread. The superposition of the two effects can be easily visualized in case of Gaussian Point Spread Function (PSF)

$$RMS = \sigma \sqrt{1 + \left(\frac{0.13^\circ}{\sigma}\right)^2}$$

where the root mean square of the signal  $RMS$  is related to the variance  $\sigma^2$  of the PSF. The contribution of the Moon size to the RMS is (not) dominant when  $\sigma$  is low (high), i.e. at high (low) particle multiplicities. Just to be explicit, the difference between

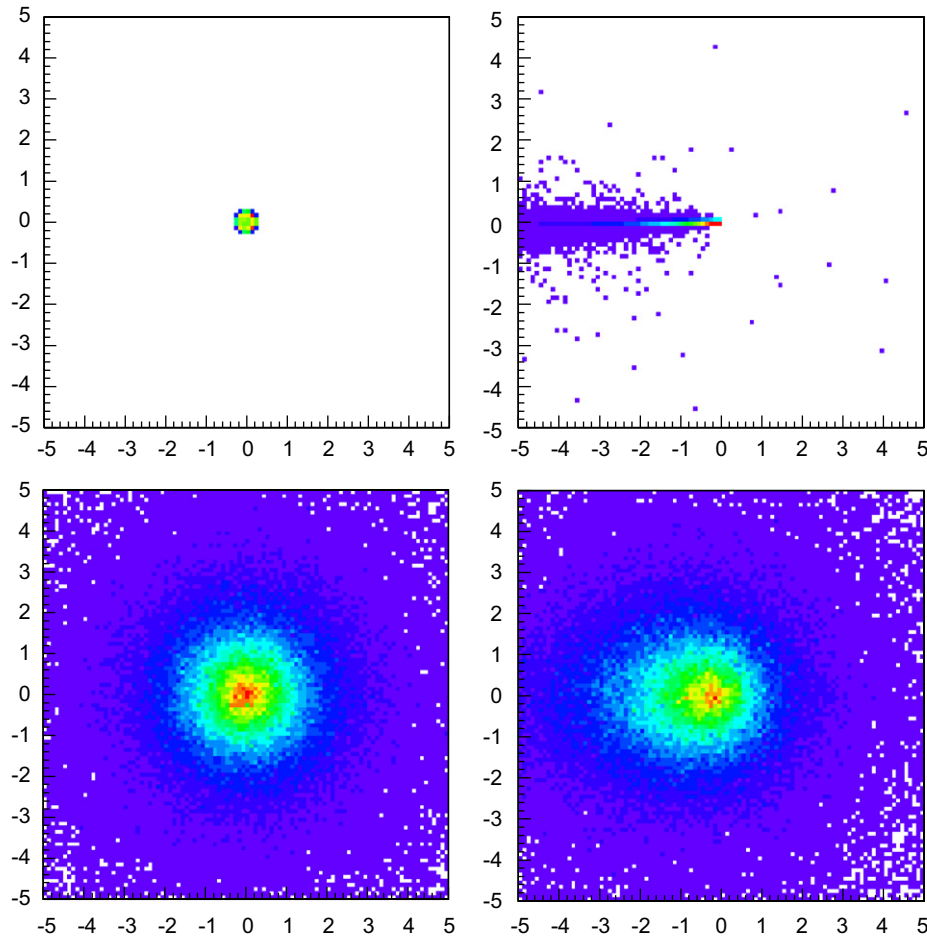


**Fig. 3.** Folding different contributions to the Moon signal. Upper part of the figure: Moon as it would be observed by a perfect detector without geomagnetic field; only the magnetic field is switched on. Lower part: only the detector is switched on; both the magnetic field and the detector are switched on. The maps are drawn using equatorial coordinates (declination VS corrected right ascension). Only the showers triggering the detector are shown ( $N > 20$ ). The color scale represents the intensity of the signal. (For interpretation of the references to color in this figure legend, the reader is referred to the web version of this article.)

RMS and  $\sigma$  is 20% if  $\sigma = 0.2^\circ$ , <5% if  $\sigma > 0.4^\circ$ , and only 1.7% if  $\sigma = 0.7^\circ$ .

Finally, it is worth to invert the switching order of the detector effect and of the geomagnetic field. In Fig. 4, the effect of the angular resolution on the East–West projection of the Moon is shown. Because of the signal asymmetry induced by the magnetic field, such an effect provides not only the smearing, but also a further displacement of the signal peak. The West tail of the shifted signal, in fact, has a larger weight than the sharp East one and tends to pull the signal in its direction.

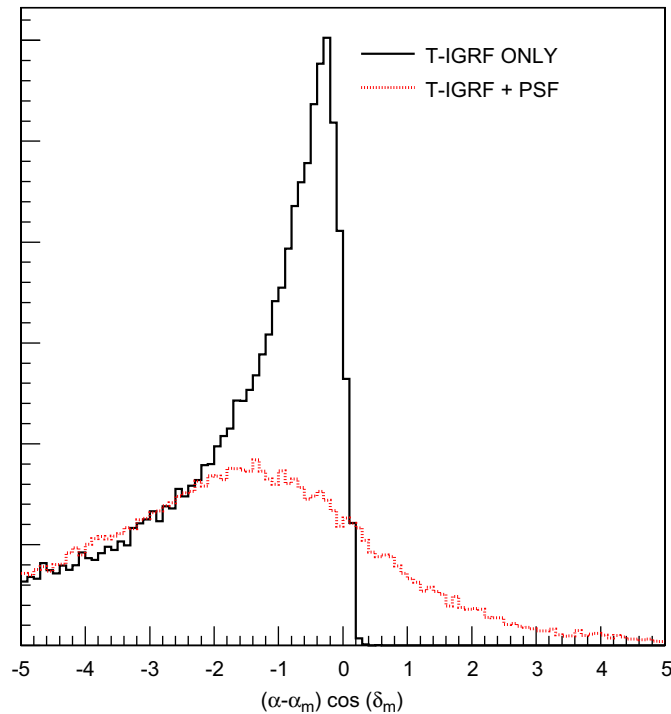


**Fig. 4.** Effect of the PSF along the east–west direction. The continuous black line represents the Moon shadow deformed by the geomagnetic field as it would appear to an ideal detector. By considering also the effect of the detector PSF, the displacement of the signal peak is enhanced, moreover the well-known smearing effect. The figures represent only protons.

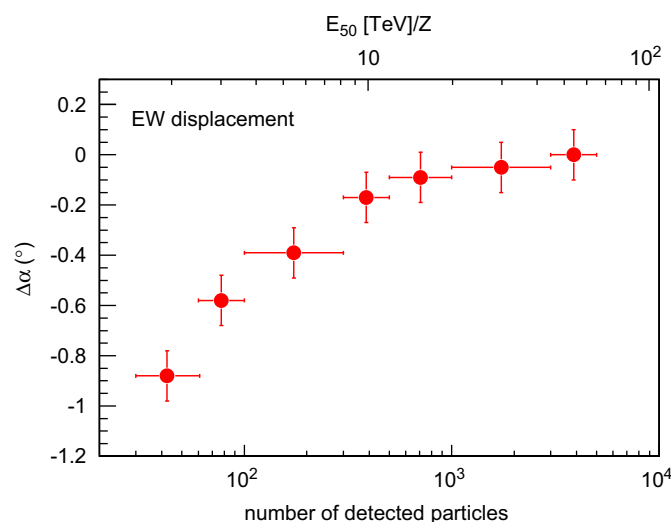


**Fig. 5.** Expected displacement of the Moon shadow in the East–West direction as a function of multiplicity. The upper scale refers to the median energy of rigidity (TeV/Z) in each multiplicity bin (shown by the horizontal errors).

In Fig. 5, the total eastward displacement is plot vs the number of detected particles.

### 3. Conclusions

We reproduced the Moon shadow effect as observed by an ideal detector located at high altitude. Much attention has been devoted to the simulation of the geomagnetic field bending the particle trajectories. We have been able to disentangle the contribution to the final signal of the geomagnetic field and of the detector PSF, respectively. We quantified the contribution of the finite Moon disc to the angular resolution estimation. For a comparison with the data collected by the ARGO-YBJ experiment, see Ref. [3].

### Appendix

Here is shown how to obtain the formula (1). Since only the magnetic field is supposed to act upon the particles trajectories, the Lorentz equation can be written as

$$\mathbf{x}(t) = \mathbf{x}_0 + \mathbf{v}_0 t + \frac{Zec^2}{E} \int_0^t d\tau \int_0^\tau d\alpha \frac{d\mathbf{x}}{d\alpha} \times \mathbf{B}(\mathbf{x}, \alpha) \quad (2)$$

where  $\mathbf{x}(t)$  is the particle position at the time  $t$ ;  $\mathbf{x}_0$  and  $\mathbf{v}_0$  are the initial position and velocity of the particle;  $Ze$  and  $E$  are its charge and its (constant) energy;  $\mathbf{B}(\mathbf{x}, t)$  is the magnetic field, which in principle can vary both with respect to the position and to the time.

If it is possible to write down an explicit functional form for  $B(\mathbf{x}, t)$ , an attempt to solve Eq. (2) can be made. On the contrary, especially when the variation with the time cannot be easily summarized with an analytical formula, a numerical solution is unavoidable.<sup>3</sup>

Eq. (2) explicitly shows the perturbation induced by the magnetic field on the straight trajectory ( $\mathbf{x}(t) = \mathbf{x}_0 + \mathbf{v}_0 t$ ). This suggests an iterative method to determine the solution, which can be expressed as the series:

$$\mathbf{x}(t) = \mathbf{x}_{O(B^0)}(t) + \mathbf{x}_{O(B^1)}(t) + \dots$$

where  $\mathbf{x}_{O(B^0)}(t) = \mathbf{x}_0 + \mathbf{v}_0 t$  is the unperturbed (straight) trajectory and for the higher orders holds

$$\Delta \mathbf{x}_{O(B^{i+1})}(t) = \frac{Zec^2}{E} \int_0^t d\tau \int_0^\tau d\alpha \frac{d\mathbf{x}_{O(B^i)}}{d\alpha} \times \mathbf{B}(\mathbf{x}_{O(B^i)}, \alpha), \quad i = 0, 1, \dots$$

where  $\Delta \mathbf{x}_{O(B^{i+1})}(t) = \mathbf{x}_{O(B^{i+1})}(t) - (\mathbf{x}_0 + \mathbf{v}_0 t)$  is the displacement from the unperturbed trajectory at the time  $t$ . Being content with the first-order approximation, it can be obtained

$$\Delta \mathbf{x}(t) \simeq \frac{Zec^2}{E} \mathbf{v}_0 \times \int_0^t d\tau \int_0^\tau d\alpha \mathbf{B}(\mathbf{x}_0 + \mathbf{v}_0 \alpha, \alpha)$$

or

$$\Delta \mathbf{x}(t) \simeq \frac{Z}{E} \mathbf{v}_0 \times \mathcal{I}_B(t; \mathbf{x}_0, \mathbf{v}_0) \quad (3)$$

where  $\mathcal{I}_B(t; \mathbf{x}_0, \mathbf{v}_0)$  is the integral of the magnetic field along the straight trajectory, whose value depends only on the time of the motion and on its initial conditions ( $\mathbf{x}_0$  and  $\mathbf{v}_0$ ).

Since the phenomenon studied concerns ultra-relativistic particles and fixing for a moment the initial position and the

<sup>3</sup> I.e. what has been done in the main part of this paper.

final time, Eq. (3) becomes

$$\Delta \mathbf{x} \simeq \frac{Z}{E} \hat{\mathbf{v}}_0 \times \mathcal{I}_{\mathbf{B}}(\hat{\mathbf{v}}_0)$$

In short, on a first approximation the displacement depends only on the ratio charge-to-energy of the primary and on the initial direction of its ultra-relativistic motion (versor  $\hat{\mathbf{v}}_0$ ).<sup>4</sup>

Let us consider only the lowest order of the geomagnetic field multipoles-expansion, i.e. the *dipole term*

$$\mathbf{B}(\mathbf{x}) = \frac{3(\mathbf{b} \cdot \mathbf{x})\mathbf{x} - \chi^2 \mathbf{b}}{\chi^5}$$

where  $\mathbf{b}$  has intensity  $b \approx 8.1 \times 10^{27} \text{ T m}^3$  and the south magnetic pole is supposed to have coordinates  $78.3^\circ$  South,  $111.0^\circ$  East. By setting  $\hat{\mathbf{v}}_0 \parallel \mathbf{x}_0$  (*vertical direction approximation*) and integrating from YangBajing to a distance  $\sim 60$  Earth's radii, Eq. (1) is immediately obtained.

## References

- [1] D. Heck, et al., Report FZKA, vol. 6019, 1998.
- [2] B. Wiebel-Sooth, et al., Astron. Astrophys. 330 (1998) 389.
- [3] R. Iuppa, et al., in: 31st ICRC, Lodz, in press.
- [4] S. Agostinelli, et al., Nucl. Instr. and Meth. A 506 (2003) 250.
- [5] M. Amenomori, et al., Astrop. Phys. 28 (2007) 137.
- [6] N.A. Tsyganenko, M.I. Sitnov, J. Geophys. Res. 112 (2007) A06225.

<sup>4</sup> The second dependence is not trivial at all. Because of the difference in the field-integrals, two identical particles having the same energy and starting together from the Moon can drift from the straight trajectory differently according to their different initial directions.